This full text paper was peer reviewed at the direction of IEEE Communications Society subject matter experts for publication in the IEEE ICC 2009 proceedings

Exploiting the Operating Point in Sensing-Based Opportunistic Spectrum Access Scenarios

X. Gelabert, O. Sallent, J. Pérez-Romero and R. Agustí
Dept. Signal Theory and Communications (TSC), Universitat Politècnica de Catalunya (UPC), Barcelona, Spain
{xavier.gelabert, sallent, jorperez,ramon}@tsc.upc.edu

***Abstract*—Spectrum sensing is one key enabler towards opportunistic spectrum access in cognitive radio networks. Such scenarios allow cognitive users (a.k.a. secondary users) to access some licensed spectrum band as long as they do not interfere with the licensed (or primary) users. The main goal is to achieve an efficient and utmost access to the otherwise underutilized spectrum resources while still guaranteeing primary users a non-harmful operation. Spectrum sensing can be then used by secondary users to detect spectrum holes that may be accessed in a non-interfering manner. However, spectrum sensing may be subject to errors in the form of false-alarm and misdetection. False-alarm causes spectrum under-use while misdetection leads to spectrum interference between primary and secondary users. Unfortunately, these two magnitudes pose a trade-off on the sensing mechanism: low misdetection is achieved at the expense of high false alarm and vice versa. Consequently, an adequate operating point of the sensing mechanism should be determined. In this work we evaluate the impact of false-alarm and misdetection errors on the performance of a spectrum sensing scenario. We use a Discrete Time Markov Chain (DTMC) model and we determine the suitable operating point for the sensing mechanism under different traffic load conditions such that some Quality of Service is attained by both primary and secondary users. Performance results reveal that by effectively choosing the operation point bearing in mind the traffic load levels will lead to enhanced perceived quality of service of both primary and secondary users.**

I. Introduction

While historically spectrum bands have been assigned following a fixed and licensed policy, current spectrum scarcity and underutilization calls for the introduction of a new communication paradigm which enables non-licensed users (secondary users) to access the licensed band in a non-harmful manner. In this sense, Cognitive Radio (CR) technologies and networks are envisaged to enable flexible and dynamic spectrum access on an opportunistic basis which have converged towards the standardization efforts by IEEE802.22 and P1900 [1], [2].

In this framework, the spectrum sharing concept deals with the problem of allowing secondary users (SUs) to access the licensed spectrum provided they do not cause interference with primary (i.e. licensed) users (PUs) which, on the other hand, have strict priority access [3]. For such operation, the secondary network must retrieve information about the primary spectrum occupancy activity in order to determine if a certain SU (or SUs) can access the shared spectrum without interfering with a PU (or PUs). The way in which this information is retrieved largely depends on the adopted architecture (infrastructure-based or infrastructure-less) and the degree of interactions between the primary and secondary network (e.g., coordinated vs. uncoordinated) [4]. Infrastructure-based secondary networks (SNs) may retrieve spectrum occupancy information from many sources which can then be made available to incumbent SUs demanding access, whereas infrastructure-less networks (e.g. ad-hoc networks) will probably rely on own measurements, e.g. by means of spectrum sensing mechanisms. If some coordination exists between primary and secondary networks, primary spectrum usage can be made available to the secondary network through e.g. common control channels as in [5], [6], [7]. Conversely, an uncoordinated primary-secondary interaction would mean that the secondary network should implement its own spectrum discovery mechanisms.

In this paper, we adopt the case that primary spectrum occupancy information is gathered by means of spectrum sensing mechanisms implemented on SUs' terminals. In such case, spectrum sensing may be affected by errors and consequently provide false information to the SU. These errors are typically in the form of false-alarm (i.e. a free channel is erroneously sensed to be occupied) and misdetection (i.e. an occupied channel is erroneously sensed to be free). As we will see, by adequately choosing the operating point of the sensing mechanism, a trade-off may be achieved between these two errors. This operating point is actually determined by the value of the decision threshold used, e.g., in energy detection mechanisms [8].

So far, and to the best of authors' knowledge, existing works in the same area mainly focus on the time devoted to sensing (*sensing time*) as a critical parameter, but pay less attention to the operation point, see e.g. [9], [10], [11]. Then, in this paper we study the impact of the sensing operating point in terms of perceived Grade of Service (GoS) for primary and secondary users and also from a global perspective. Such study is carried out using a Discrete Time Markov Chain (DTMC) framework developed by the authors in [4]. Results indicate that effectively choosing the operation point will lead to enhanced perceived quality of service of both PUs and SUs.

This work was performed in project E^3 which has received research funding from the Community's Seventh Framework program. This paper reflects only the authors' views and the Community is not liable for any use that may be made of the information contained therein. The contributions of colleagues from E^3 consortium are hereby acknowledged. This work has been supported by the Spanish Research Council and FEDER funds under COGNOS grant (ref. TEC2007-60985).

978-1-4244-3435-0/09/$25.00 ©2009 IEEE

This paper is organized as follows. Section II presents the considered spectrum sensing model and defines the sensing operation point. A brief description of the DTMC model is provided in Section III and the definition of Grade-of-Service metrics in Section IV. In Section V some performance results are shown and conclusions are derived in Section VI.

II. Spectrum Sensing Model Formulation

In this work we assume that spectrum sensing over a given band is performed using energy detection techniques [8]. Such method consists in measuring the energy of the received waveform over a given bandwidth W (Hz) and an observation time-window T (s). The product $m = T \cdot W$ is usually referred to as the time-bandwidth product. Several works, among them [8], [12], have been devoted to determine closed-form analytical expressions for the false-alarm and misdetection (or detection) probabilities under various channel conditions. Basically, energy detection performs a binary hypothesis on the occupancy of a band or channel: $\mathcal{H}_0$ if the channel is free and $\mathcal{H}_1$ if the channel is occupied. Then, the false-alarm and misdetection, ε and δ accordingly, can be defined as:

$$\varepsilon = \Pr\left[Y > \lambda | \mathcal{H}_0 \text{ is true}\right] \triangleq G_\varepsilon(\lambda) \quad (1)$$

$$\delta = \Pr\left[Y < \lambda | \mathcal{H}_1 \text{ is true}\right] \triangleq G_\delta(\lambda)\,, \quad (2)$$

where the decision statistic Y is compared to the decision threshold λ so as to determine the occupancy status of the channel. Accordingly, expressions for $G_\varepsilon(\lambda)$ and $G_\delta(\lambda)$ can be found accounting for several channel conditions and cooperation schemes, see citeDigham,Ghasemi for further details.

Of particular interest is to determine the relation between ε and δ through the so-called *Receiver Operating Characteristic* (ROC) curves where ε is plotted against δ for some given average signal-to-noise ratio (γ) and time-bandwidth product (m). Formally, from (1) we can express $\lambda = G_\varepsilon^{-1}(\varepsilon)$ and by using (2) we obtain $\delta = G_\delta\left(G_\varepsilon^{-1}(\varepsilon)\right)$ which results in the ROC curve in Fig. 1a. Each point over such curve, hereon indicated by the pair $(\delta_0, \varepsilon_0)$, denotes a possible operating point (OP) for the sensing mechanism. Note the existing trade-off between false-alarm and misdetection probability where low values of ε are attained at high values of δ and vice versa.

By appropriately selecting a specific decision threshold value $\lambda = \lambda_0$ we obtain a particular value for the OP $(\delta_0, \varepsilon_0)$. It is worth mentioning that the function mapping between λ_0 and $(\delta_0, \varepsilon_0)$ is bijective, i.e., there is a one-to-one correspondence between λ_0 and $(\delta_0, \varepsilon_0)$ values in both directions.

For the sake of representation, rather than using the decision threshold λ (which depends on the decision statistic Y and, consequently, on the measured signal energy) we define the *operating-point mix* Θ, with $0 \leq \Theta \leq 1$, as:

$$\Theta \triangleq \frac{\log(\varepsilon/\varepsilon_{\min})}{\log(\delta/\delta_{\min}) + \log(\varepsilon/\varepsilon_{\min})}\,, \quad (3)$$

where $\varepsilon_{\min}$ and $\delta_{\min}$ are the minimum operating values for the false-alarm and misdetection probabilities respectively given

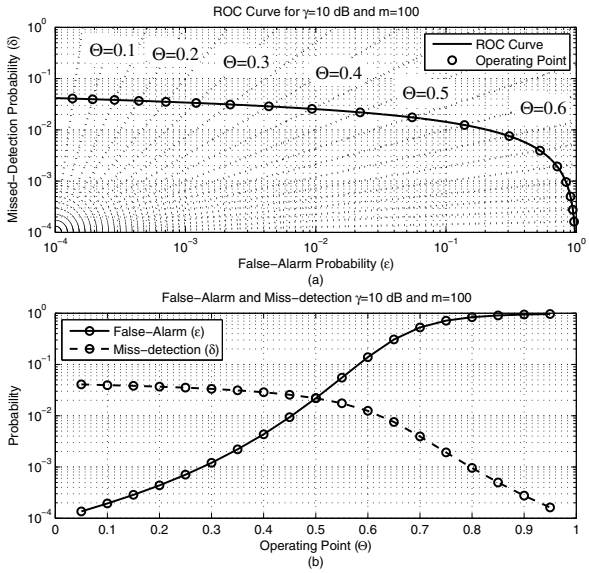

Fig. 1: (a) ROC curves in Rayleigh fading channel and (b) tradeoff between false-alarm and miss-detection against the operating point.

by the ROC curve (see that $\varepsilon_{\min} = \delta_{\min} = 10^{-4}$ in Fig. 1a). The values of $\varepsilon_{\min}$ and $\delta_{\min}$ can be regarded as the resolution of the sensing mechanism and consequently they are determined by the sensing equipment characteristics. Then, after some algebra manipulation, it follows that:

$$\delta = \delta_{\min}\left(\varepsilon/\varepsilon_{\min}\right)^{\left(\frac{1}{\Theta}-1\right)}\,, \quad (4)$$

which is plotted in Fig. 1a, for different values of $0 \leq \Theta \leq 1$, which results in the set of dashed lines crossing the origin of coordinates at $(\delta_{\min}, \varepsilon_{\min})$. For each particular value of $\Theta = \Theta_0$ we obtain a particular OP $(\delta_0, \varepsilon_0)$ which is represented by the circles in Fig. 1a denoting the intersection of the line equation given by (4) with the ROC curve.

In this way, we have a normalized parameterization through parameter Θ for the feasible OPs of the sensing mechanism. Note that, see Fig. 1b, for $0 < \Theta < 0.5$ we have that $\delta > \varepsilon$; for $\Theta = 0.5$ we obtain $\delta = \varepsilon$; and finally, for $0.5 < \Theta < 1$ we have $\delta < \varepsilon$. Then, the value of Θ will be used to represent the full range of cases and determine, for different traffic conditions, which is the most suitable OP.

III. DTMC Model Formulation

The proposed DTMC model accounts for the spectrum occupancy of PUs and SUs in a shared spectrum scenario. Due to space limitations, only a brief description of the model will be provided here. For a comprehensive and more detailed exposition, the reader is referred to [4] by the authors.

The considered spectrum model assumes a given spectrum bandwidth partitioned into C channels (bands) to be shared among both PUs and SUs. It is further assumed that both PUs and SUs demand a single channel for transmission purposes. In addition, a SU is able to release a channel which is suddenly

occupied by a PU and move to another channel, provided there is a free one, or interrupt its session otherwise.

In a DTMC we observe the system state at discrete time instants $\{t_0, t_1, t_2, ..., t_n, ...\}$, with $t_n = t_0 + n \cdot \Delta T$ and periodicity ΔT, which is, moreover, assumed to specify the sensing periodicity. If $N_p(t_n)$ and $N_s(t_n)$ are stochastic processes indicative of the number of PUs and SUs in the system at time t_n, then, let $\mathbf{X}_n = S_{(i,j)} = \{N_p(t_n) = i, N_s(t_n) = j\}$ represent a state of the DTMC at time t_n. We may consequently consider the state space $\mathcal{S}$ of our model as the set of states such that $\mathcal{S} = \left\{S_{(i,j)} : i \leq C, j \leq C\right\}$ where, additionally, the non-collision state space $\mathcal{S}_{nc} = \left\{S_{(i,j)} : i + j \leq C\right\}$ and the collision state space $\mathcal{S}_c = \left\{S_{(i,j)} : i + j > C\right\}$ can be defined.

Due to spectrum sensing errors, the observed state at time t_n may be $\mathbf{Y}_n = S_{(k,j)} \in \mathcal{S}$, such that $\mathbf{Y}_n \neq \mathbf{X}_n$, with k denoting the number of sensed PUs. Consequently, it can be shown (here omitted for the sake of space), that the conditional probability of sensing k PUs when there are actually i PUs at time t_n is:

$$b_{(k,i)} = \sum_{m=\max(0,i-k)}^{\min(i,C-k)} \binom{C-i}{m+k-i} \cdot \varepsilon^{m+k-i} \cdot \bar{\varepsilon}^{C-m-k} \cdot \binom{i}{m} \cdot \delta^{m} \cdot \bar{\delta}^{i-m}, \quad (5)$$

with $\bar{\varepsilon} \triangleq 1 - \varepsilon$ and $\bar{\delta} \triangleq 1 - \delta$.

According to (5), false-alarm and misdetection, ε and δ, will affect the sensed number of PUs by the SN, thus potentially causing erroneous decisions due to the inaccuracy of spectrum awareness information. Accordingly, the DTMC model will capture such effects yielding a more realistic scenario description compared to known approaches so far.

For a complete formulation of the DTMC model, it is necessary to define the expressions for the $S_{(i,j)} \rightarrow S_{(k,l)}$ state transition probabilities $P_{(i,j|k,l)}$. These probabilities are the entries of the transition probability matrix, $\mathbf{P}$, from which the steady state probabilities, $P_{(i,j)}$, of the DTMC will be determined. In addition, the steady state probabilities of the sensed states $P'_{(i,j)}$ (i.e. including possible sensing errors) can also be determined. Since such definitions are already provided in [4], and thus not adding substantial novelty to this paper, the reader is referred to [4] for a complete and detailed definition of the state transition probabilities and the derivation of the steady state probabilities $P_{(i,j)}$ and $P'_{(i,j)}$.

IV. Grade of Service in Opportunistic Spectrum Access Scenarios

In this work the impact of the OP on the performance of PUs and SUs is addressed. To this end, we adopt the classical Grade-of-Service (GoS) concept in wireless networks [13] and adapt it to the opportunistic spectrum access scenario. GoS metrics, shown hereafter, will be computed from the steady state probabilities $P_{(i,j)}$ and $P'_{(i,j)}$ obtained from the DTMC.

Primary GoS (GoS^P) is derived from the blocking and interference probabilities affecting PUs as follows[1]:

$$GoS^P = \left(P_B^P + \omega_P \cdot P_I\right) / (1 + \omega_P), \quad (6)$$

with $\omega_P > 1$ a weight factor indicating that interference is more hazardous than the blocking from the PUs' perspective. Primary blocking probability (P_B^P) and interference probability (P_I) are accordingly defined as:

$$P_B^P = \sum_{j=0}^{C} P_{(C,j)} \quad (7)$$

$$P_I = \sum_{S_{(i,j)} \in \mathcal{S}_c} P_{(i,j)}. \quad (8)$$

As for secondary GoS (GoS^S), we consider the blocking probability along with the interruption probability (i.e. the probability that a SU is forced to evacuate a channel due to primary activity) such that we define:

$$GoS^S = \left(P_B^S + \omega_S \cdot P_D^S\right) / (1 + \omega_S), \quad (9)$$

with $\omega_S > 1$ the corresponding secondary weight factor indicating that interruption is more harmful than blocking. Accordingly, the secondary blocking (P_B^S) and interruption probability (P_D^S) are defined as:

$$P_B^S = \sum_{i=0}^{C} \sum_{j=C-i}^{C} P'_{(i,j)} \quad (10)$$

and

$$P_D^S = 1 - N_S / \left[T_S \cdot \left(1 - P_B^S\right)\right], \quad (11)$$

with T_S the offered secondary traffic and N_S the average number of SUs given by:

$$N_S = \sum_{S_{(i,j)} \in \mathcal{S}} j \cdot P_{(i,j)}. \quad (12)$$

Finally, we may define the aggregate GoS as:

$$GoS^A = \left(GoS^S + \omega_A \cdot GoS^P\right) / (1 + \omega_A), \quad (13)$$

which jointly accounts for the individual GoS of both PUs and SUs and where we consider that weight factor $\omega_A > 1$ will prioritize PU quality since they have strict precedence as licensed users of the shared spectrum. Note that ω_P, ω_S and ω_A should be chosen adequately in accordance to the expected perceived GoS of each user type (i.e. PU or SU). Nevertheless, notice that these values are empirical and depend on the subjective perception of the grade of service.

V. Results

We consider the total bandwidth partitioned into $C = 16$ channels. Performance evaluation is carried out against several primary and secondary traffic conditions. Firstly, hereon denoted as SMIX1, the offered primary traffic load is fixed with value $T_P = \lambda_P / \mu_P = 5$ Erlangs whereas secondary traffic, T_S, is chosen so that the service-mix, defined as $\sigma = T_P / (T_P + T_S)$ (with $0 < \sigma < 1$), ranges between

[1]For convenience, a normalized version of the $GoS \in [0, 1]$ is used, where $GoS \rightarrow 1$ means degraded operation while $GoS \rightarrow 0$ means improved operation.

0.1 and 0.9 (in steps of 0.1). In addition, hereon denoted as SMIX2, it is assumed the case of secondary traffic load fixed to $T_S = \lambda_S/\mu_S = 5$ Erlangs and primary traffic load T_P, is determined so that the service-mix σ also ranges between 0.1 and 0.9. Spectrum sensing periodicity is $\Delta T = 1$ seconds and the time-bandwidth product is fixed (unless otherwise stated, u.o.s.) with value $m = 100$ (as in Fig. 1). Weighting factors for GoS computation in (6), (9) and (13) are set to $\omega_P = \omega_S = 10$ and $\omega_A = 30$ (u.o.s.), where we indicate that interference and interruption penalize more than blocking, and that primary GoS is prioritized over secondary GoS.

A. Traffic Dependency

Fig. 2a shows the primary GoS for the SMIX1 case. Given that the offered primary load ($T_P = 5$ Erlangs) is relatively low compared to the number of channels ($C = 16$), the GoS degradation is mainly due to the interference probability which is particularly hazardous when $\Theta \to 0$. Recall from Fig. 1b that when $\Theta \to 0$ we incur in high misdetection, thus SUs are more likely to access a channel already occupied by a PU, thus causing interference. This effect is more noticeable for increased secondary traffic loads as reflected in Fig. 2a. Fig. 2b shows the secondary GoS, again, for the SMIX1 case. In this case, the behavior is opposite of that of primary GoS. Indeed, secondary GoS benefits from low false-alarm (i.e. $\Theta \to 0$) given that less interruption probability is attained in this case. On the other hand, for $\Theta \to 0$ blocking rises due to an excess of SUs spectrum access; and for $\Theta \to 1$ blocking rises due to high false alarm which prevents SU accessing the spectrum. Since secondary GoS is a weighted metric that penalizes interruption probability more than blocking (recall $\omega_S = 10$ in (9)), the observed performance is that of 2b, where $\Theta \to 1$ implies secondary GoS degradation.

Fig. 2c shows the aggregate GoS for the SMIX1 case where it can be seen that the most suitable OP, i.e. the one that provides the lowest aggregate GoS, depends on the offered secondary traffic load. Indeed, for low secondary load, the OP may be pushed towards $\Theta \to 0$ which benefits both primary and secondary GoSs (see Fig. 2a and Fig. 2b). Whereas for higher secondary traffic loads (about $T_S = 7.5$ Erlangs), $\Theta \to 0$ values would imply worse primary GoS and thus $\Theta \to 1$ is required since primary GoS is prioritized.

In addition, Fig. 3 shows the GoS for primary, secondary and aggregate for the case of SMIX2. In this case, an analogous discussion follows as pointed out for Fig. 2. Primary GoS in Fig. 3a, as previously indicated, benefits from $\Theta \to 1$ values since it implies lower misdetection probabilities which in turn cause interference. In addition, for high primary traffic loads ($T_P = 11.67$ Erlangs) the primary GoS is degraded due to high blocking probability. As for secondary GoS in Fig. 3b, a similar behavior to that of Fig. 2b is noted. Indeed, a degradation of secondary GoS is noticed as the primary traffic load increases (given they have priority), and also when $\Theta \to 1$ due to a rise in secondary blocking caused by excessive false-alarm events. Finally, in Fig. 3c the aggregate GoS is shown. It is observed that, as long as primary traffic load is kept low, values of $\Theta \to 0$ which benefit SUs can be considered. However, as primary load rises, and given PUs have priority over SUs, values benefiting PUs, i.e. $\Theta \to 1$, are required.

Given Figs. 2c and 3c, we are able to choose the most suitable OP value, Θ, for different traffic load conditions according to the displayed function $GoS^A(\Theta)$. In this sense, note that in some situations a suitable value for Θ (i.e. that minimizes the perceived aggregate GoS) spans over a given range while under other traffic conditions, a single suitable Θ value can be considered. We are then interested in determining the *feasible* OP region, defined as the range of Θ values such that aggregate GoS, $GoS^A(\Theta)$, is at most a Δ_Θ percent higher than the minimum, which is $GoS^A(\Theta^*)$, and where Θ^* indicates the OP where the aggregate GoS is minimum. Formally, the *feasible Operating Point region* is defined as:

$$\mathcal{F}_\Theta = \left\{\Theta : GoS^A(\Theta) \leq GoS^A(\Theta^*) \cdot (1 + \Delta_\Theta/100)\right\} \quad (14)$$

The value of Δ_Θ will determine how stringent are our GoS requirements and where the smaller its value the more stringent those requirements are.

Accordingly, Fig. 4 shows the feasible OP region for $\Delta_\Theta = 0.1\%$ and $\Delta_\Theta = 0.01\%$ (shaded in different grey tones). Consider the traffic conditions of SMIX1 (for SMIX2 a similar approach can be applied which is omitted here for the sake of brevity). Note that for $\Delta_\Theta = 0.01\%$ tighter upper and lower limits are obtained for the feasible region as compared to the case of $\Delta_\Theta = 0.01\%$, thus indicating higher constraints on feasible Θ values. As for Fig. 4, note that, as long as secondary traffic is kept at reduced limits (i.e. service-mix σ below approx. 0.4) such that the interference caused to PUs is low a wide range of OP values will still provide good GoS to both PUs and SUs. Recall that SUs benefit from $\Theta \to 0$ values and that PUs are satisfied with $\Theta \geq 0.6$ (see Fig. 2a). However, if secondary traffic is increased beyond some point (i.e. service mix higher approximately than 0.6), then primary GoS is at jeopardy and thus a narrowed range of OP values is feasible, while $\Theta \to 0$ values are not accepted any longer.

B. Signal-to-Noise Ratio Dependency

As mentioned in Sec. II, the performance of the sensing mechanism, in terms of false-alarm and misdetection, and hence the OP, will be affected, among other parameters, by the perceived signal-to-noise ratio (SNR). Accordingly, Fig. 5 shows the feasible operating point region for $\Delta_\Theta = 0.1\%$ and $\Delta_\Theta = 0.01\%$. Traffic conditions are $T_P = 5$ Erlangs and $T_S = 11.67$ Erlangs and the time-bandwidth product is $m = 100$. It can be observed that lower SNR values imply a much more narrowed feasible OP region than higher SNR values indicating that, in harsh conditions, the operating point should be chosen in a more precise way. In addition, for higher SNRs, the feasible region is somewhat more flexible allowing a less stringent OP value, and thus a wider feasible region is observed. This is particularly noticeable for $\Delta_\Theta = 0.1\%$ which is less strict than $\Delta_\Theta = 0.01\%$. In contrast, a slight increase of the feasible OP value is noted in for $\Delta_\Theta = 0.01\%$ when SNR>8dB. This is due to the fact that increased SNR

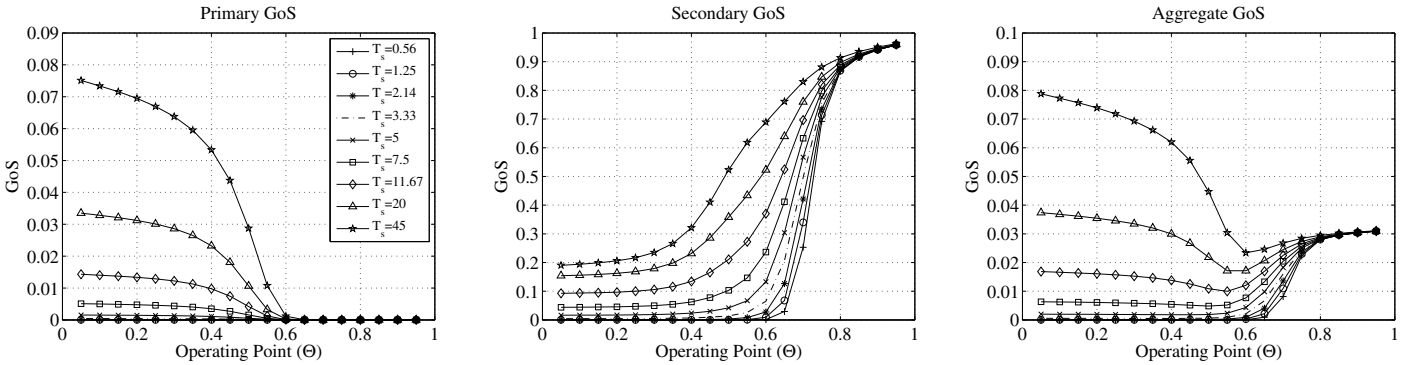

Fig. 2: Results for SMIX1: (a) Primary GoS, (b) Secondary GoS, and (c) Aggregate GoS, against operating-point Θ.

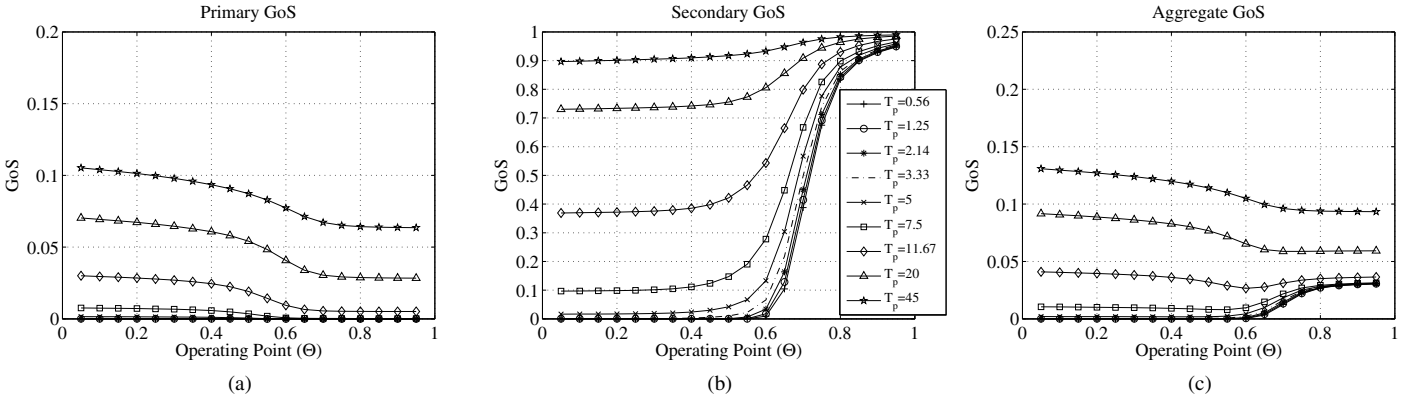

Fig. 3: Results for SMIX2: (a) Primary GoS, (b) Secondary GoS, and (c) Aggregate GoS, against operating-point Θ.

values will improve detection of white holes and therefore SUs are more likely to access the shared spectrum. Consequently, the interference probability increases due to these SUs and the primary GoS is degraded. To combat this effect, and since primary GoS is prioritized over secondary GoS, the OP needs to be increased so that the misdetection probability decreases.

C. Time-Bandwidth Product Dependency

The time-bandwidth product (m) is yet another parameter influencing the performance of the sensing mechanism. In this sense, in Fig. 6 we plot the feasible OP region for different values of m. The overall behavior is somewhat analogous to the dependency with the SNR. Indeed, an increase of m (and thus the time devoted to sensing purposes) is translated into a better discovery of free channels by the SUs. Therefore, higher chances that SUs access the shared spectrum happen, which in turn translates into higher interference probability with the PUs. Consequently, a slight increase in the suitable OP when m increases is observed in order to "protect" PUs from excessive interference. This is particularly visible for $\Delta_\Theta = 0.01\%$, since more stringent GoS is required.

D. Scenario Characterization through Parameter ω_A

By setting the values of ω_A in (13), several scenarios can be characterized according to the level of "willingness" by the licensee towards secondary opportunistic access. Then, high values of ω_A indicate higher protection for PUs, thus a conservative approach, whereas low values of ω_A indicate a more relaxed opportunistic access to the shared resources. In this sense, the feasible OP region has been plotted in Fig. 7 for a range of ω_A values. In Fig. 7a by setting $\omega_A = 1$ we indicate that no precedence is offered to primary GoS with respect to secondary GoS. Therefore, when secondary load increases (i.e. $\sigma \to 0$), secondary GoS is severely penalized with respect to primary GoS (see Fig. 2a and 2b), then $\Theta \to 1$ OP values are necessary to improve secondary GoS. If we increase ω_A, denoting that higher precedence is offered to primary users, some trends may be observed in Figs. 7a to 7d. In the first place, the upper limit of the feasible OP region increases towards $\Theta \to 1$ when ω_A increases. This happens because, in order to protect primary GoS, higher OP values are needed which ensure lower misdetection and thus lower interference probability. Secondly, as long as secondary traffic is kept sufficiently low, still OP values of $\Theta \to 0$ are allowed since primary GoS is not seriously affected in these cases.

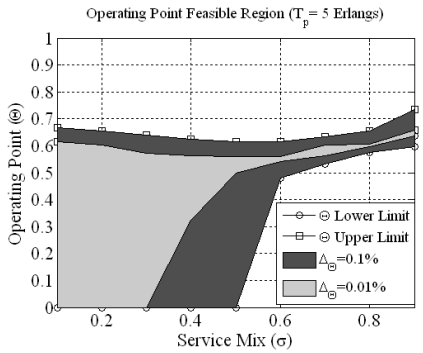

Fig. 4: Feasible OP regions varying traffic conditions for SMIX1.

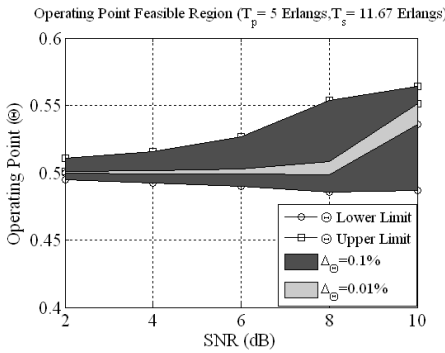

Fig. 5: Feasible OP regions varying SNR conditions.

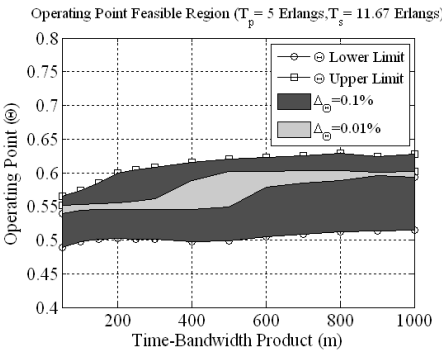

Fig. 6: Feasible OP regions varying the time-bandwidth product.

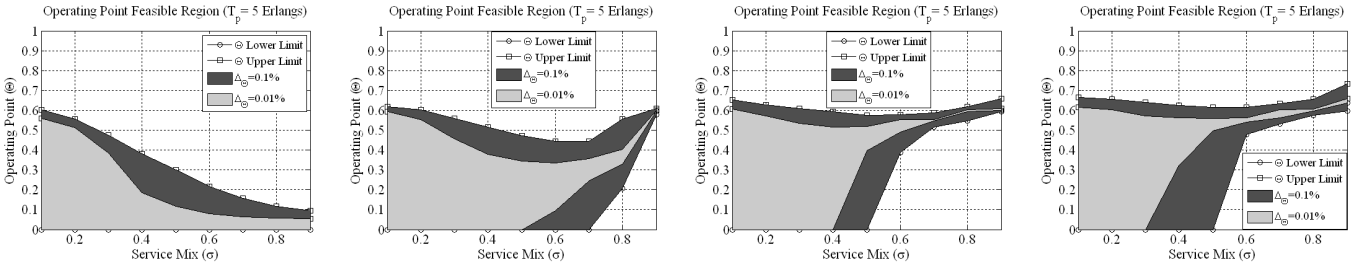

(a) (b) (c) (d)

Fig. 7: Feasible OP regions for SMIX1 varying scenario (a) $\omega_A = 1$, (b) $\omega_A = 10$, (c) $\omega_A = 40$, and (d) $\omega_A = 100$.

However, when secondary traffic becomes large, increased OP values are needed in order to protect the PUs. This is observed by noting that the non-feasible OP region in lower-right corner of Figs. 7a to 7d gets larger with ω_A.

VI. Conclusion

Spectrum sensing is a key enabler for opportunistic access to shared spectrum environments. In this work, we have exploited the operating point of spectrum sensing mechanisms in order to improve the perceived GoS of both primary and secondary users. Results indicate that improved and efficient sensing operation can be obtained bearing in mind current traffic load and SNR conditions. In this sense, specific sensing operating point values can be determined within feasible OP regions, thus offering the possibility of automatically adapting the decision threshold to traffic varying scenarios and thus achieving improved secondary operation while non-interfering on primary spectrum usage. In addition, primary/secondary spectrum access characterization has been evaluated according to the "willingness" of the licensee towards secondary opportunistic access. Results indicate that the sensing operating point should be considered as a relevant design parameter when evaluating spectrum sharing scenarios.

References

[1] C. Cordeiro, K. Challapali, D. Birru, and N. Sai Shankar, "IEEE 802.22: the first worldwide wireless standard based on cognitive radios," in *IEEE DySPAN'05*, Nov. 2005, pp. 328–337.

[2] M. Muck et al., "IEEE P1900.B: Coexistence Support for Reconfigurable, Heterogeneous Air Interfaces," in *IEEE DySPAN'07*, Apr. 2007, pp. 381–389.

[3] R. Etkin, A. Parekh, and D. Tse, "Spectrum sharing for unlicensed bands," in *IEEE DySPAN'05*, Nov. 2005, pp. 251–258.

[4] J. Pérez-Romero, X. Gelabert, O. Sallent, and R. Agustí, "A novel framework for the characterization of dynamic spectrum access scenarios," in *IEEE PIMRC'08*, Sept. 2008.

[5] J. Pérez-Romero, O. Sallent, R. Agustí, and L. Giupponi, "A Novel On-Demand Cognitive Pilot Channel Enabling Dynamic Spectrum Allocation," in *IEEE DySPAN'07*, Apr. 2007, pp. 46–54.

[6] M.M. Buddhikot et al., "DIMSUMnet: new directions in wireless networking using coordinated dynamic spectrum," *IEEE WoWMoM'05*, pp. 78–85, June 2005.

[7] D. Raychaudhuri and X. Jing, "A spectrum etiquette protocol for efficient coordination of radio devices in unlicensed bands," in *IEEE PIMRC'03*, vol. 1, Sept. 2003, pp. 172–176 Vol.1.

[8] F. Digham, M.-S. Alouini, and M. Simon, "On the energy detection of unknown signals over fading channels," *IEEE ICC'03*, vol. 5, pp. 3575–3579 vol.5, May 2003.

[9] A. Ghasemi and E. S. Sousa, "Optimization of spectrum sensing for opportunistic spectrum access in cognitive radio networks," in *IEEE CCNC'07*, Jan. 2007, pp. 1022–1026.

[10] Y.-C. Liang, Y. Zeng, E. Peh, and A. T. Hoang, "Sensing-throughput tradeoff for cognitive radio networks," *IEEE Trans. Wireless Commun.*, vol. 7, no. 4, pp. 1326–1337, April 2008.

[11] W.-Y. Lee and I. F. Akyildiz, "Optimal spectrum sensing framework for cognitive radio networks," *IEEE Trans. Wireless Commun.*, vol. 7, no. 10, pp. 3845–3857, October 2008.

[12] A. Ghasemi and E. Sousa, "Collaborative spectrum sensing for opportunistic access in fading environments," in *IEEE DySPAN'05*, Nov. 2005, pp. 131–136.

[13] J. Zander and S.-L. Kim, *Radio Resource Management for Wireless Networks*. Norwood, MA, USA: Artech House, Inc., 2001.